I would like to express my gratitude to the editor and reviewers for their invaluable comments, which have been of great value in enhancing the quality of the manuscript content and correcting the author's writing errors due to inadvertence. In response to all the comments, all revisions have been marked in the resubmitted manuscript. We have marked the changes to the original manuscript.

Reviewer #1

General comments:

1. The specific data quality control procedures for POSP (e.g., cloud detection, outlier removal) remain unclear in the manuscript, potentially affecting result reproducibility. It is recommended to supplement detailed descriptions of POSP data preprocessing steps (e.g., cloud masking, pixel screening criteria) and clarify their impacts on the matching strategy.

Thank you for pointing this out. We overlooked the description of the data preprocessing step, and we appreciate your reminder, which is very helpful in improving the quality of the manuscript. Since the algorithm proposed in this study is specifically designed for cloud-free land pixels, we removed land pixels that might contain clouds or ice/snow before retrieval. When retrieval pixels contain potential cloud contamination, the results tend to be significantly overestimated. A strict cloud detection process can effectively mitigate this issue. Additionally, to ensure the reliability of the validation, we adopted the following matching strategies:

“satellite data are averaged over a 3 × 3 window centered on the AERONET site, and ground-based observations are averaged over a 30-minutes window before and after the time of satellite overpass. To mitigate the uncertainty associated with averaged data, a minimum of two or more ground-based observations are required in the temporal matching window, and the spatial matching window must encompass more than three valid satellite observation pixels”

A detailed description of the preprocessing has been added to the Methods section.

“As an optical sensor, POSP observations are inherently susceptible to cloud interference. To mitigate cloud contamination, it is essential to filter out cloud-affected pixels prior to retrieval. Given the single-angle observation characteristics of POSP, this study adopts cloud detection strategies from MODIS, which have been extensively validated. Specifically, two methods are employed: the apparent reflectance threshold method and the apparent reflectance spatial variation detection method (Martins et al., 2002). The former effectively identifies optically thick clouds with high reflectance or substantial water vapor content, while the latter is particularly useful for detecting cloud edges, shadows, thin clouds, and dispersed cloud formations.

Additionally, surface conditions such as snow and water also affects the inversion. Since the retrieval algorithm is explicitly designed for clear-sky, non- ice & water land surfaces, observations over water, ice, and snow must be excluded. The detection of snow and water pixels is achieved using the Normalized Difference Water Index (NDWI) and the Normalized Difference Snow/Ice Index (NDSI), respectively, with specific identification thresholds represented in Table 1.

$$NDWI = \frac{\rho_{670} - \rho_{865}}{\rho_{670} + \rho_{865}} \quad (9)$$

$$NDSI = \frac{\rho_{670} - \rho_{2250}}{\rho_{670} + \rho_{2250}} \quad (10)$$

While the aforementioned cloud detection strategy provides a foundation for minimizing cloud contamination, there remains potential for further improvement. Given the relatively coarse spatial resolution of POSP (6.4 km) and its limited spectral coverage, certain pixel which contains cloud fragments may remain undetected. To enhance cloud-mask accuracy, a dedicated cloud detection algorithm for POSP is still needed. We will further enhance the cloud detection algorithm in future work.

Table 1 Summary of screening thresholds.

Items	Purpose
$\rho_{443} < 0.02\ or\ \rho_{443} > 0.4$	Cloud
$\sigma_{443} > 0.038$	Cloud
$\rho_{1380} > 0.02\ and\ Height < 1500$	Cloud
$\sigma_{1380} > 0.005$	Cloud
$NDWI > 0$	Water
$NDSI > 0.4$	Snow/Ice

"

2. Line24, Lines 178-182: The significant underestimation in high-AOD regions (e.g., North Africa) is attributed to "aerosol model errors" without specific analysis of discrepancies between model assumptions and actual aerosol characteristics. Further investigation into aerosol model classification and its impact on retrieval errors is suggested.

We sincerely apologize for any misunderstanding caused by our oversight. First, Fig. 15 in the manuscript shows that POSP AOD exhibits a significant overestimation compared to MODIS DB AOD over North Africa and the Arabian Peninsula. However, when compared to MODIS MAIAC AOD, POSP AOD appears much closer in these regions. Since both MAIAC AOD and DB AOD are official MODIS products, the large discrepancy between them highlights the complexity of aerosol retrievals. Overall, POSP AOD aligns well with MAIAC AOD over North Africa and the Arabian Peninsula, while it is more consistent with DB AOD in other regions.

In recent years, the global ground-based observation network has expanded significantly, improving coverage in many areas. However, ground-based observations remain sparse in remote and inaccessible regions. Given the current distribution of ground-based observation sites, it remains challenging to determine which aerosol product achieves the highest accuracy globally compared to others.

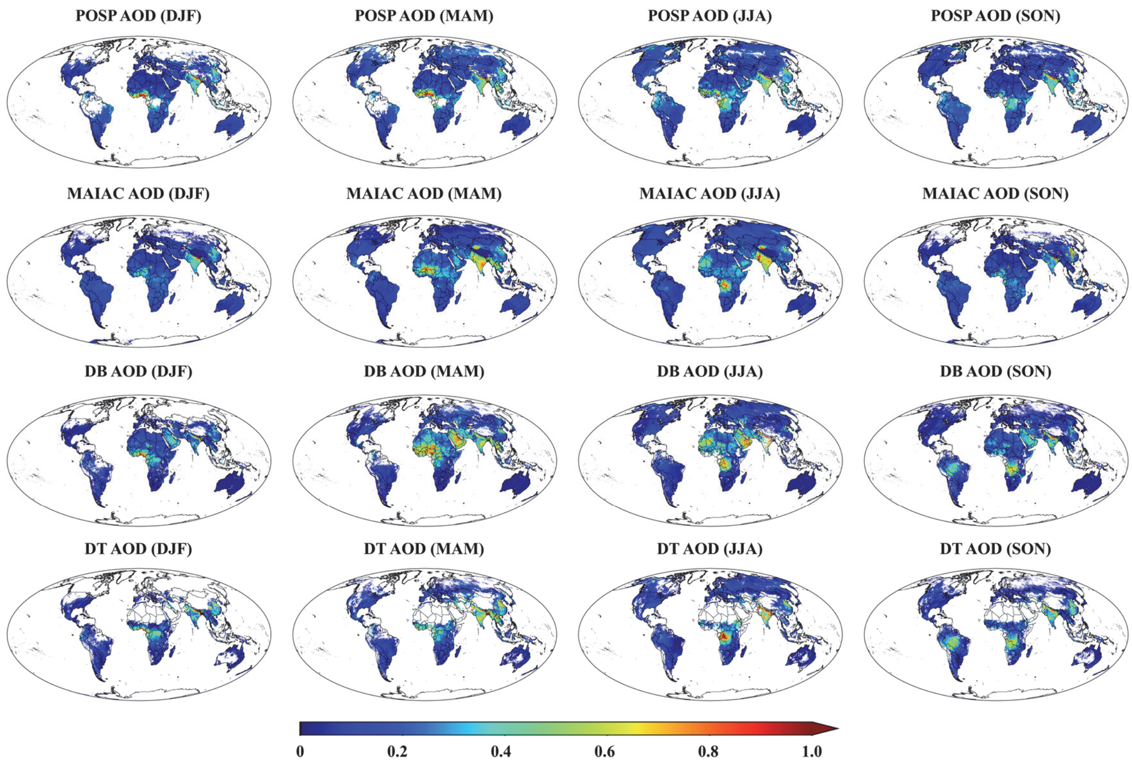

Figure 1: Maps of the seasonally averaged AOD derived from POSP, MODIS MAIAC, MODIS DB and MODIS DT, for the winter (DJF: December–January–February), spring (MAM: March–April-May,) summer (JJA: June–July–August), and autumn (SON: September–October–November).

This study performs retrievals based on a fixed aerosol model, which may lead to significant discrepancies between the assumed and actual aerosol models. Li et al. (2018) have quantitatively described the impact of aerosol model error on retrieval accuracy through simulation experiments. They applied the optimal estimation theory and calculated the degree of freedom for signal (DFS) available for aerosol retrieval parameters to quantify their information content (Frankenberg et al., 2012; Hasekamp and Landgraf, 2005). This method has been widely used to assess the theoretical retrieval capability of sensors.

Here, the aerosol model errors correspond with the combination of 6 predefined aerosol parameters $\{r_{eff}^{f},\ v_{eff}^{f},\ r_{eff}^{c},\ v_{eff}^{c},\ m_{i}^{f},\ m_{i}^{c}\}$, which are all assumed to change from 5% to 100% by a step of 5% with the constant measurement error, as well as the constant a priori errors of m_i^f and m_i^c. r_{eff}^f and r_{eff}^c represent the effective radius of fine- and coarse-mode aerosol, respectively. v_{eff}^f and v_{eff}^c represent the effective variance of fine- and coarse- mode aerosol, respectively. m_i^f and m_i^c represent the refractive index of fine- and coarse- mode aerosol, respectively. It is evident that as the aerosol model error increases, DFS decreases linearly, indicating that the retrieval uncertainty correspondingly increases.

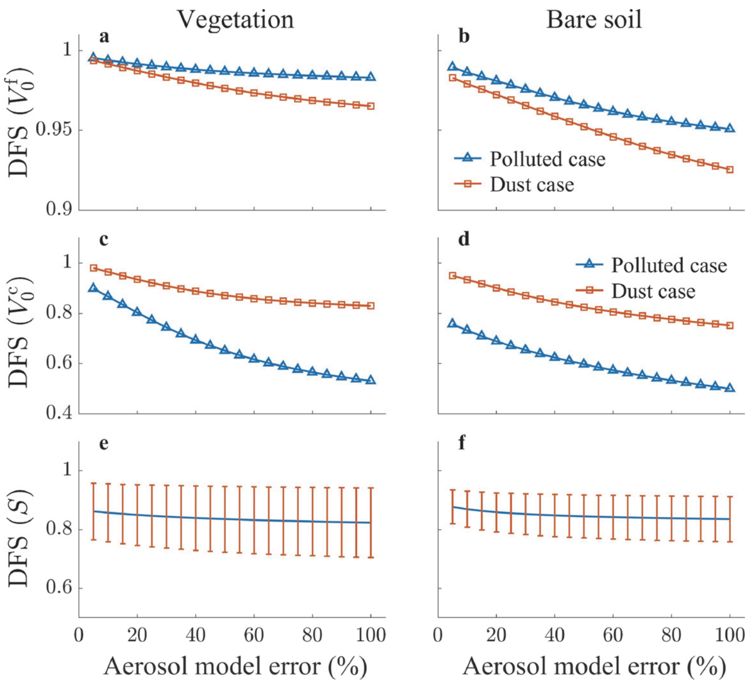

Fig. 13. Same as Fig. 11 but for as a function of the aerosol model errors from 5% to 100% by a step of 5% with AOD= 0.6.

We have added descriptions in the relevant sections regarding the impact of aerosol model error on retrieval accuracy.

"The accuracy of POSP AOD decreases at high AOD, which may be attributed to the increasing aerosol model error. As AOD increases, the impact of discrepancies between the assumed aerosol model and the actual aerosol model is amplified, leading to an increase in retrieval uncertainty (Hou et al., 2018; Li et al., 2018)."

" On the other hand, POSP AOD shows high consistency with AERONET AOD in heavily polluted regions such as northern India, central and western Africa, and central South America, although the GCOS fraction is lower. This is because, as AOD increases, the influence of the surface on retrieval accuracy decreases, while the influence of the aerosol model increases. Thus, using a fixed aerosol model inevitably affects the accuracy of retrievals (Levy et al., 2013). This is one of the inherent challenges of intensity retrieval with single-angle observations, and we will gradually address this issue in future algorithm improvements."

3. Lines 302-304: The explanation for lower AOD accuracy in urban areas remains overly generalized ("complex surface and diverse pollution components"), lacking quantitative analysis (e.g., interference from urban surface reflectance anisotropy). Enhanced discussion on separating urban surface reflectance from aerosol signals is recommended.

Thank you very much for pointing this out. Your comment is extremely valuable for improving the quality of our manuscript. We acknowledge that our analysis lacked a detailed discussion on the impact of urban surface reflectance anisotropy on aerosol retrievals. Therefore, we have now included a comprehensive discussion on this aspect, as detailed below.

"To further explore the impact of urban surface reflectance anisotropy on aerosol retrievals, we separated the urban surface reflectance from aerosol signals. First, based on the global BRDF kernel results obtained through spectral reconstruction by Ji et al. (2025), Table 2 presents the BRDF results for urban in 2022, extracted using the global land cover classification product MCD12C1. A subsequent clustering analysis categorized the global urban BRDF kernel coefficients into seven classes.

Figs. 8 and 9 illustrate the surface reflectance which was computed using Eqs. S1-S9 at 443 nm and 490 nm, respectively (the solar zenith angle was set at 30°). Since the retrieval algorithm ultimately considers only the apparent reflectance at 443 nm and 490 nm, simulations were limited to these bands. The simulations show that the surface reflectance increases significantly when the view zenith angle exceeds approximately 75°. However, the actual retrieval only utilizes observations with view zenith angles below 60°, thereby avoiding this issue. Furthermore, it is evident that surface reflectance increases notably when the view zenith angle approaches the sun zenith angle, corresponding to the maximum scattering angle.

Finally, we simulated the apparent reflectance under observation geometries and AOD following a Gaussian distribution (sun zenith angle from 10° to 70°; view zenith angle from 0° to 60°; relative azimuth angle from 0° to 360°; AOD from 0 to 1.5). To simulate aerosol conditions over cities, we used a mixture of continental and dirty aerosol types in equal proportions (50% each) following Omar et al. (2009). Notably, to account for real-world observational conditions, we introduced random errors to the simulated apparent reflectance consistent with calibration accuracy.

Table 2 BRDF kernel coefficients statistics for different urban types.

Kernal name	Band (nm)	Type 1	Type 2	Type 3	Type 4	Type 5	Type 6	Type 7
Isotropic	443	0.068	0.044	0.053	0.104	0.076	0.049	0.127
	490	0.083	0.055	0.065	0.123	0.091	0.060	0.150
volumetric	443	0.017	0.021	0.017	0.028	0.041	0.036	0.058
	490	0.021	0.024	0.022	0.033	0.048	0.042	0.067
geometric-optical	443	0.016	0.010	0.011	0.023	0.014	0.007	0.020
	490	0.020	0.013	0.013	0.027	0.017	0.009	0.023

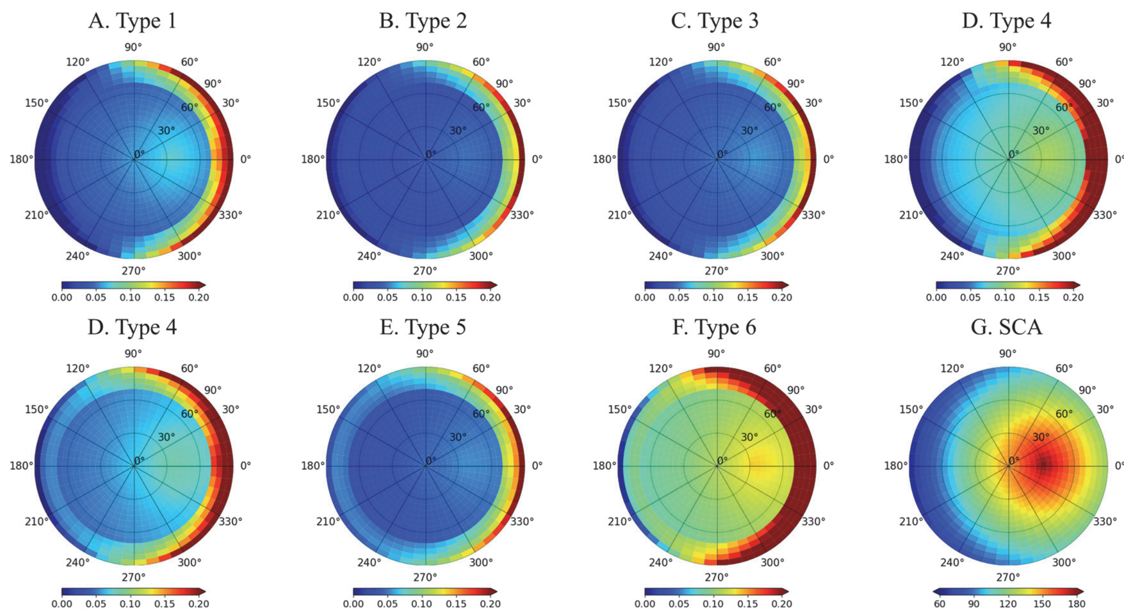

Figure 2: The polar plots of the BRDF distribution for urban surface. (A)-(F) The result of surface reflectance at 443 nm, and (G) The scattering angle plot. In this polar plot, the radius denotes a change in view zenith angle from 0° to 90°, and the polar angle represents a change in relative azimuth angle from 0° to 360°. The simulations are performed at a solar zenith angle of 30°.

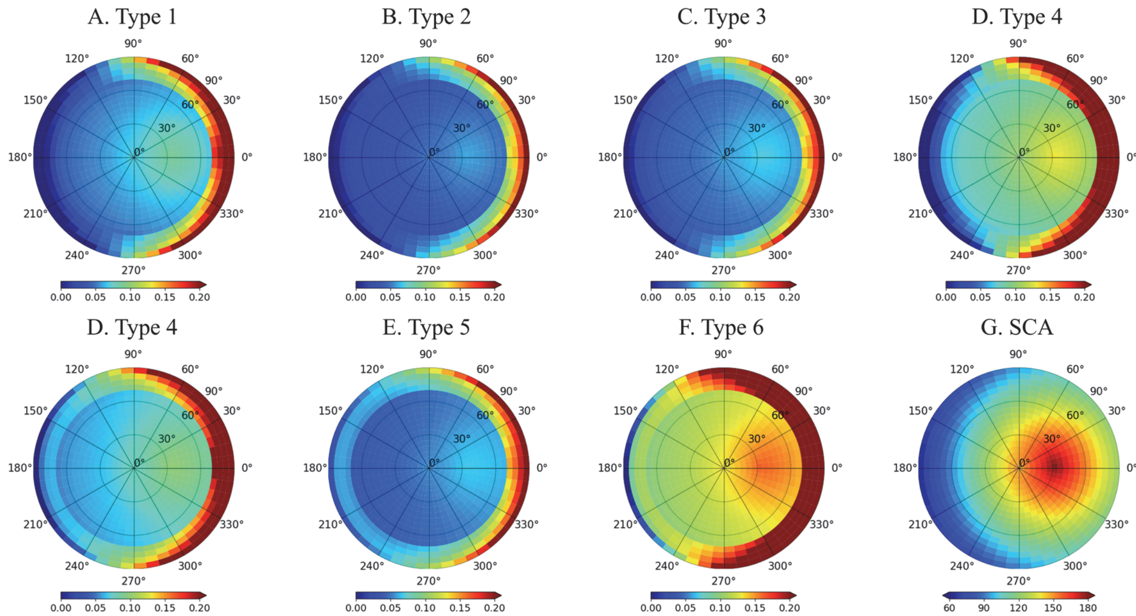

Figure 3: The same as Fig.8, but the. surface reflectance at 490 nm.

First, we calculated the apparent reflectance using the non-Lambertian forward radiative transfer model in Eqs. S10-S11 and then performed the retrieval using the Lambertian forward radiative transfer model in Eq. S12. To isolate the effect of surface reflectance anisotropy on retrievals, we used the same aerosol model in the forward simulation for retrieval.

Fig. S7 in the supplementary document shows that neglecting surface anisotropy leads to an overestimation of apparent reflectance, leading to the underestimation for aerosol retrieval. For type 4 and 7 which has the highest reflectance, this overestimation is most pronounced, indicating that the higher the surface reflectance, the greater the impact of ignoring surface anisotropy on retrieval accuracy.

Figs. 10 and 11 illustrate how retrieval errors caused by neglecting surface anisotropy vary with scattering angle and aerosol loading. Because of overestimation of simulated apparent reflectance using Lambertian forward radiative transfer model, the retrieved AOD is underestimated. Overall, as AOD increases, the impact of ignoring surface anisotropy on retrievals diminishes, and this effect is noticeable when surface reflectance is high. In fact, for type 2 and 3 which has the lowest reflectance surfaces, the retrieval error caused by neglecting surface anisotropy remains nearly constant across different aerosol loading. Retrieval errors also slightly increase as the scattering angle increases.

In general, the impact of surface reflectance magnitude on retrieval errors is more significant than the influence of AOD or scattering angle. Therefore, for aerosol retrievals over urban, the effect of surface anisotropy on retrieval accuracy is non-negligible in regions with high surface reflectance.

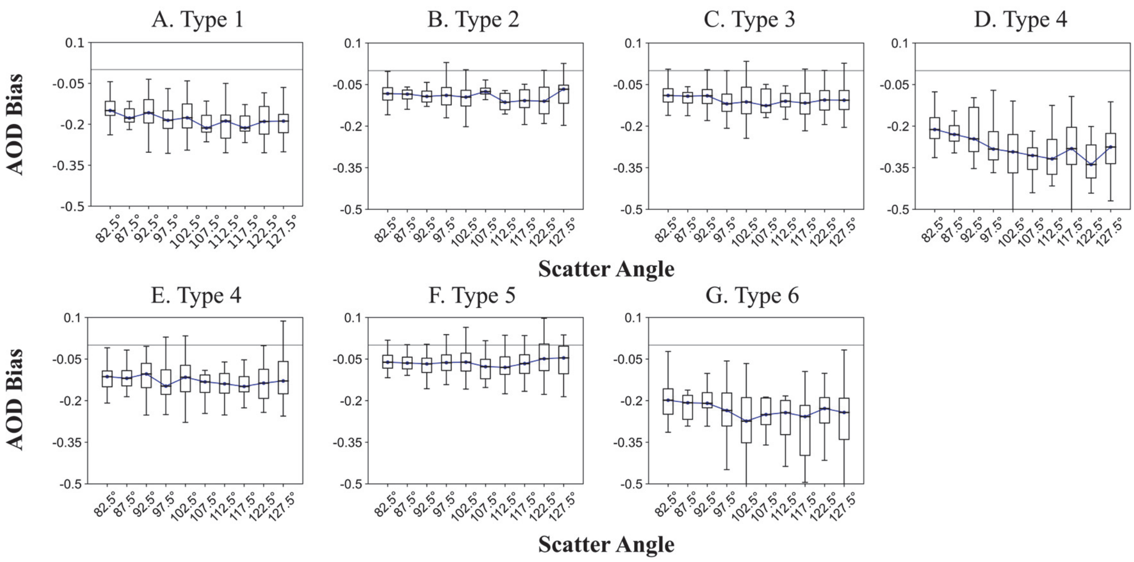

Figure 4: AOD bias as function of scattering angle for different urban surface type.

Figure 5: The same as Fig 10, but AOD bias as function of aerosol loading.

”

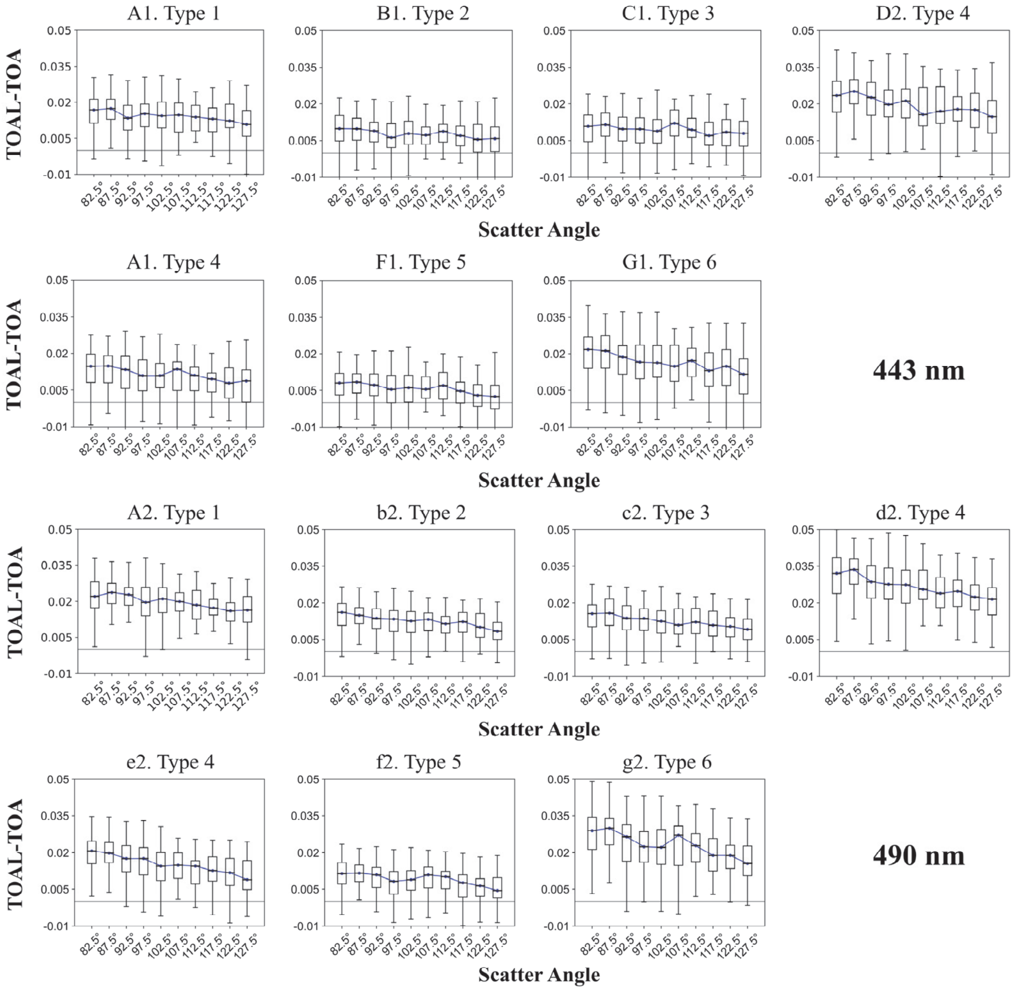

Figure S6: The boxplot of the differences for apparent reflectance between the results calculated based on the Lambertian forward radiative transfer model (TOAL) and the non-Lambertian forward radiative transfer model (TOA). The upper panel shows the differences as a function of AOD, while the lower panel presents the differences as a function of the scattering angle.

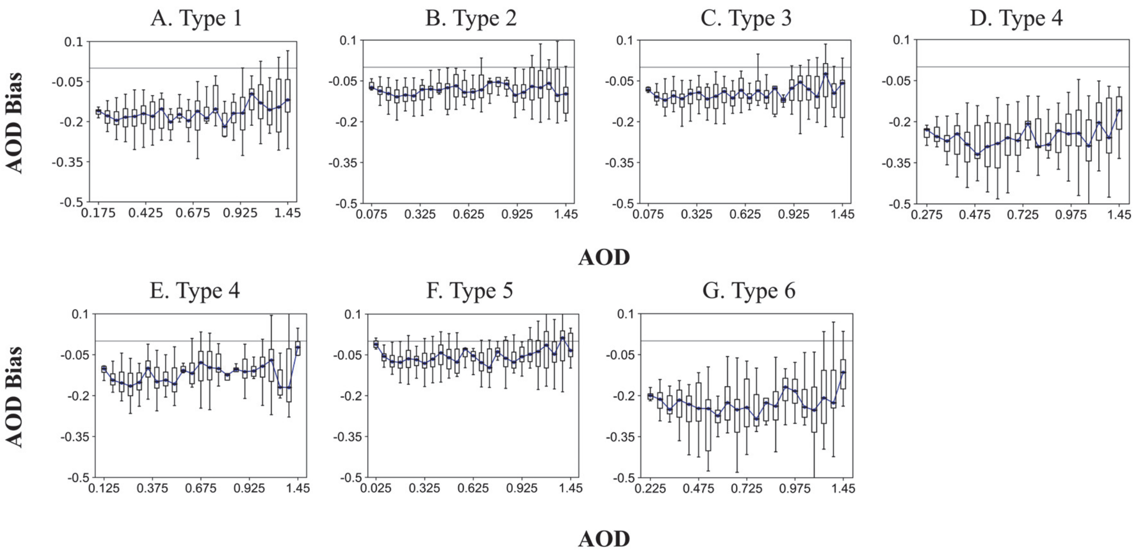

Figure S7: AOD bias as function of aerosol loading for different urban surface type.

4.Line 246:"Other LC types which are not shown in Fig.4 are presented in Fig. S1." Figs. S1-S9 need to be found in the supplementary document. It is recommended to describe clearly in the manuscript.

We apologize for any inconvenience caused by our description. We have revised the relevant sections to make the explanation as clear as possible.

5.Some grammatical inconsistencies exist. Comprehensive language polishing is advised to ensure proper tense usage and grammatical consistency throughout the manuscript.

We sincerely apologize for any inconvenience caused. We have invited Professor Gerrit de Leeuw, an expert in the field of aerosols remote sensing, to revise our manuscript for grammatical errors and further improve the quality of the manuscript.

Reviewer #2

General comments:

References

Frankenberg, C., Hasekamp, O., O'Dell, C., Sanghavi, S., Butz, A., and Worden, J.: Aerosol information content analysis of multi-angle high spectral resolution measurements and its benefit for high accuracy greenhouse gas retrievals, Atmospheric Measurement Techniques, 5, 1809–1821, 2012.

Hasekamp, O. P. and Landgraf, J.: Retrieval of aerosol properties over the ocean from multispectral single-viewing-angle measurements of intensity and polarization: Retrieval approach, information content, and sensitivity study, Journal of Geophysical Research: Atmospheres, 110, 2005.

Hou, W., Li, Z., Wang, J., Xu, X., Goloub, P., and Qie, L.: Improving Remote Sensing of Aerosol Microphysical Properties by Near-Infrared Polarimetric Measurements Over Vegetated Land: Information Content Analysis, Journal of Geophysical Research: Atmospheres, 123, 2215–2243, 2018.

Ji, Z., Ma, Y., de Leeuw, G., Shi, Z., and Li, Z.: An Enhanced Aerosol Optical Depth Retrieval Algorithm for Particulate Observing Scanning Polarimeter (POSP) Data Over Land, IEEE Trans. Geosci. Remote Sensing, 63, 1–18, https://doi.org/10.1109/TGRS.2024.3514170, 2025.

Levy, R. C., Mattoo, S., Munchak, L. A., Remer, L. A., Sayer, A. M., Patadia, F., and Hsu, N. C.: The Collection 6 MODIS aerosol products over land and ocean, Atmos. Meas. Tech., 6, 2989–3034, https://doi.org/10.5194/amt-6-2989-2013, 2013.

Li, Z., Hou, W., Hong, J., Zheng, F., Luo, D., Wang, J., Gu, X., and Qiao, Y.: Directional Polarimetric Camera (DPC): Monitoring aerosol spectral optical properties over land from satellite observation, Journal of Quantitative Spectroscopy and Radiative Transfer, 218, 21–37, https://doi.org/10.1016/j.jqsrt.2018.07.003, 2018.

Martins, J. V., Tanré, D., Remer, L., Kaufman, Y., Mattoo, S., and Levy, R.: MODIS cloud screening for remote sensing of aerosols over oceans using spatial variability, Geophysical Research Letters, 29, MOD4-1, 2002.

Omar, A. H., Winker, D. M., Vaughan, M. A., Hu, Y., Trepte, C. R., Ferrare, R. A., Lee, K.-P., Hostetler, C. A., Kittaka, C., Rogers, R. R., Kuehn, R. E., and Liu, Z.: The CALIPSO Automated Aerosol Classification and Lidar Ratio Selection Algorithm, Journal of Atmospheric and Oceanic Technology, 26, 1994–2014, https://doi.org/10.1175/2009JTECHA1231.1, 2009.